



HAL
open science

S-wave Superconductivity in Optimally Doped SrTi $1-x$ Nb x O 3 Unveiled by Electron Irradiation

Xiao Lin, Willem Rischau, Cornelis van Der Beek, Benoît Fauqué, Kamran Behnia

► **To cite this version:**

Xiao Lin, Willem Rischau, Cornelis van Der Beek, Benoît Fauqué, Kamran Behnia. S-wave Superconductivity in Optimally Doped SrTi $1-x$ Nb x O 3 Unveiled by Electron Irradiation. Physical Review B: Condensed Matter and Materials Physics (1998-2015), 2015, Physical Review B, 92, pp.174504. 10.1103/PhysRevB.92.174504 . hal-01242476

HAL Id: hal-01242476

<https://hal.science/hal-01242476>

Submitted on 12 Dec 2015

HAL is a multi-disciplinary open access archive for the deposit and dissemination of scientific research documents, whether they are published or not. The documents may come from teaching and research institutions in France or abroad, or from public or private research centers.

L'archive ouverte pluridisciplinaire **HAL**, est destinée au dépôt et à la diffusion de documents scientifiques de niveau recherche, publiés ou non, émanant des établissements d'enseignement et de recherche français ou étrangers, des laboratoires publics ou privés.

S-wave Superconductivity in Optimally Doped $\text{SrTi}_{1-x}\text{Nb}_x\text{O}_3$ Unveiled by Electron Irradiation

Xiao Lin,¹ Carl Willem Rischau,^{1,2} Cornelis J. van der Beek,² Benoît Fauqué,¹ and Kamran Behnia¹

(1) *Laboratoire de Physique et d'Etude des Matériaux (CNRS/ESPCI/UPMC), Paris, F-75005, France*

(2) *Laboratoire des Solides Irradiés (CNRS-CEA/DSM/IRAMIS), Ecole Polytechnique, 91128 Palaiseau cedex, France*

(Dated: July 2, 2015)

We report on a study of electric resistivity and magnetic susceptibility measurements in electron irradiated $\text{SrTi}_{0.987}\text{Nb}_{0.013}\text{O}_3$ single crystals. Point-like defects, induced by electron irradiation, lead to an almost threefold enhancement of the residual resistivity, but barely affect the superconducting critical temperature (T_c). The pertinence of Anderson's theorem provides strong evidence for a s-wave superconducting order parameter. Stronger scattering leads to a reduction of the effective coherence length (ξ) and lifts the upper critical field (H_{c2}), with a characteristic length scale five times larger than electronic mean-free-path. Combined with thermal conductivity data pointing to multiple nodeless gaps, the current results identify optimally doped $\text{SrTi}_{1-x}\text{Nb}_x\text{O}_3$ as a multi-band s-wave superconductor with unusually long-range electrostatics.

PACS numbers: 74.62.Dh, 74.25.Ha, 74.25.fc

Scattering mixes the superconducting order parameter at separate points on the Fermi surface. As a consequence, one can probe changes in the two-particle wavefunction by tuning disorder. Its effect on the superconducting transition provides an opportunity to explore the symmetry of the superconducting gap. According to Anderson's theorem, in a conventional s-wave superconductor the critical temperature (T_c) is insensitive to non-magnetic disorder [1]. On the other hand, in superconductors with non-trivial gap symmetry, e.g., cuprates [2–4], Sr_2RuO_4 [5], and heavy fermions [6], T_c is extremely sensitive to potential scattering and the superconducting ground state can be completely destroyed by disorder [7–10]. In multi-band superconductors such as MgB_2 and iron pnictides, interband scattering rather than intraband scattering plays a key role in suppressing T_c and the effect of disorder depends on the ratio of interband to intraband scattering matrix elements [11–13].

Chemical substitution can be used to introduce disorder. In cuprates, T_c is drastically suppressed by Zn doping, providing strong evidence for d-wave symmetry [2]. Particle irradiation provides an alternative avenue of creating artificial defects without introducing any foreign ions. In $\text{YBa}_2\text{Cu}_3\text{O}_{7-\delta}$, scattering induced by electron irradiation suppressed T_c in a manner similar to Zn substitution [4, 14, 15]. On the other hand, in the s-wave superconductor MgB_2 , superconductivity is robust with respect to electron irradiation [16–18]. However, neutron and α -particle irradiation of MgB_2 led to an apparent suppression of T_c [19–21]. The shape and size of defects, which influence scattering, depend on the type of irradiation. Energetic heavy ions generate columnar defects along the ion trajectories [22–24]. Protons, α -particles, and neutrons most likely produce defect clusters of nm size [11]. On the other hand, high energy electrons (1–10 MeV) generate point-like defects in the form

of interstitial-vacancy pairs (Frenkel pairs) [25]. This makes electron irradiation a suitable method for introducing controlled disorder.

A band insulator with an energy gap of 3.2 eV, SrTiO_3 , is close to a ferroelectric instability aborted due to quantum fluctuations [26]. Its huge permittivity at low temperature leads to a very long Bohr radius and a precocious metallicity. Three conducting bands, composed of Ti t_{2g} orbitals and centered at the Γ point can be successfully filled by n-doping [27]. A superconducting dome, with a peak $T_c \simeq 450$ mK [28–32] exists between charge carrier densities of 3×10^{17} to 3×10^{20} cm^{-3} .

The symmetry of the superconducting order parameter has been barely explored in this system. In 1980, Binnig and co-authors detected two distinct superconducting gaps by planar tunneling measurements [33]. However, a recent tunneling experiment did not detect multiple gaps on the superconducting $\text{LaAlO}_3/\text{SrTiO}_3$ interface [34]. More recently, thermal conductivity measurements found multiple nodeless gaps in optimally doped $\text{SrTi}_{1-x}\text{Nb}_x\text{O}_3$ single crystals, paving the way for the identification of the symmetry of the superconducting order parameter [35]. A latest study reported the existence of electron pairs well beyond the superconducting ground state in quantum dots fabricated on the $\text{LaAlO}_3/\text{SrTiO}_3$ interface [36]. In this paper, we present a study of ac susceptibility and resistivity in $\text{SrTi}_{1-x}\text{Nb}_x\text{O}_3$ irradiated with high energy electrons and provide unambiguous evidence for s-wave superconductivity. We also find an intriguing signature of nonlocal electrostatics, which may be related to the long effective Bohr radius of the parent insulator of this dilute superconductor.

The $\text{SrTi}_{1-x}\text{Nb}_x\text{O}_3$ ($x=0.013$) single crystals used in this study were obtained commercially as the one used in thermal conductivity measurements [35]. Four samples with size of $5 \times 2.5 \times 0.5$ mm have been cut from the same

single crystal and gold was evaporated on their surface to make Ohmic contacts. Three of them were irradiated with 2.5 MeV electrons at the SIRIUS accelerator facility of the Laboratoire des Solides Irradiés. Irradiations were performed at 20 K in liquid hydrogen to obtain a uniform distribution of point defects in the material. After irradiation, the samples were stored in liquid nitrogen to avoid room temperature annealing of the irradiation-induced defects. The resistivity and Hall effect around the superconducting transition temperature were measured with a standard four probe method in a dilution refrigerator within a few days after the irradiation. The transport properties were rechecked in a Quantum Design PPMS system above 2 K a few months later. The Hall carrier density and residual resistivity have barely changed with time. Gold contacts that are large compared to the size of the samples may give rise to an uncertainty of 10% in the transport measurements. Finally, the ac susceptibility was measured in a homemade set-up, which consisted of one primary field coil and one compensating pick-up coil with two sub-coils with their turns in opposite direction. The exciting ac current was supplied and the induced voltage signal was picked up by a Lock-in amplifier. The applied ac magnetic field was as low as 10 mG, with frequencies between 2000 and 4000 Hz.

Fig. 1(a) shows the temperature dependence of the resistivity of the pristine sample #1 and of samples #2, #3 and #4 that were irradiated to total electron doses $Q = 300, 460$ and 1320 mC/cm² respectively. The residual resistivity $\rho_0 = \rho(2K)$ amounts to $71 \mu\Omega\text{cm}$ in the pristine sample and increases with increasing irradiation dose. The increase is caused by enhanced elastic scattering due to the point-like defects induced by the electron irradiation. Fig. 1(b) plots the Hall resistivity as a function of the magnetic field at 10 K. The Hall carrier concentration (n_H) plotted in Fig. 1(c) remains around $2.1 \times 10^{20} \text{ cm}^{-3}$ with an error of 10%, deduced from $R_H = 1/n_H e$ where $R_H = \rho_{yx}/B$ is the Hall coefficient. As seen in the figure, while the carrier concentration does not show any substantial change, ρ_0 increases linearly with the irradiation dose, indicating that the magnitude of the scattering rate is affected by the increased quantity of irradiation-induced scattering centers. ρ_0 amounts to $175 \mu\Omega\text{cm}$ in sample #4, enhanced by $104 \mu\Omega\text{cm}$ compared to #1, a magnitude comparable to what has been attained in other studies of impurity effects in superconductors such as cuprates [2] and pnictides [11]. The mean-free-path (l) can be extracted using $l = \hbar\mu k_F/e$, where \hbar and e are the fundamental constants, μ is the Hall mobility and k_F the Fermi wave factor, calculated from the carrier density assuming an isotropic single-component Fermi surface. With increasing Q , l decreases from 50 to 19 nm.

Fig. 2 shows the superconducting transition in different samples such as observed through the real part of the susceptibility (χ') and the resistivity (normalized by its normal-state magnitude). There is a smooth transition in ρ/ρ_n and the resistivity vanishes at a critical temperature ($T_{c-\rho}$) of 435 mK. On the other hand, χ' moni-

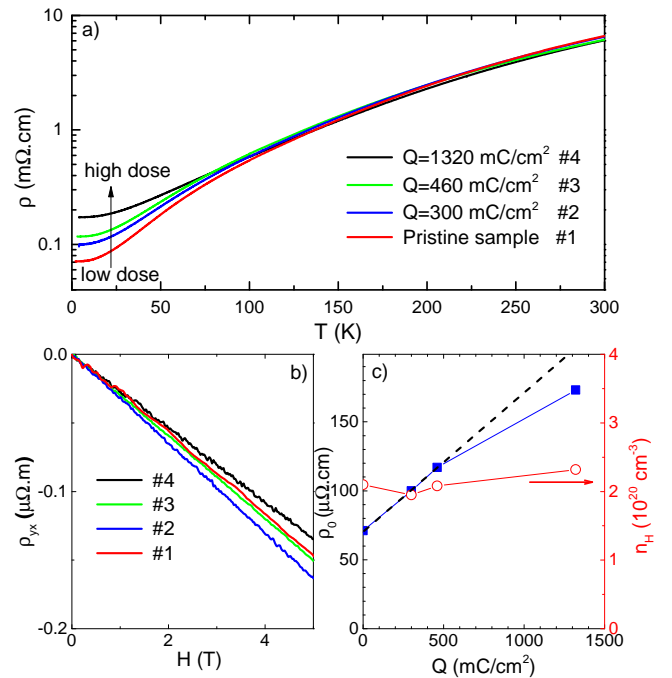


FIG. 1: Resistivity and Hall coefficient in pristine and electron-irradiated SrTi_{0.987}Nb_{0.013}O₃ single crystals. a) Temperature dependence of resistivity (note the vertical log scale). The low temperature resistivity monotonically increases with irradiation dose. b) Hall resistivity (ρ_{yx}) as a function of magnetic field at 10K. c) Residual resistivity ($\rho_0 = \rho(2K)$) and Hall carrier concentration (n_H) as a function of irradiation dose (Q). Irradiation enhances the residual resistivity by a factor of 2.5, but leaves the carrier density virtually unchanged ($n_H \approx 2.1 \times 10^{20} \text{ cm}^{-3}$). The dashed line is a guide to the eyes.

tors bulk superconductivity, i.e., full flux exclusion. The bulk superconducting transition occurs at a temperature $T_{c-\chi'}$, determined as the crossing point of two linear extrapolations, close to 370 mK. Such a difference of 65 mK between $T_{c-\rho}$ and $T_{c-\chi'}$ is comparable to what was reported in our previous study comparing the specific heat, the thermal conductivity and the resistive superconducting transitions [35]. As seen in the figure, both $T_{c-\rho}$ and $T_{c-\chi'}$ remain basically the same in the four samples. This is the principal result of this study. In spite of the significant decrease of the charge-carrier mean-free-path, the critical temperature remains the same. Neither the width of the transition nor the superconducting shielding fraction are affected by the irradiations. Table 1 lists $T_{c-\rho}$ and $T_{c-\chi'}$.

Figs. 3(a) and (b) plot $\chi'(T)$ near T_c in presence of magnetic field for samples #1 and #4. As expected, the application of a magnetic field shifts the superconducting transition to lower temperatures. In Fig. 3(c), H_{c2} is plotted as a function of $T_c/T_c(0T)$ for all the samples. A remarkable effect of the irradiation is to induce an enhancement of the slope of the upper critical field near T_c . One can quantify this effect by extracting the effec-

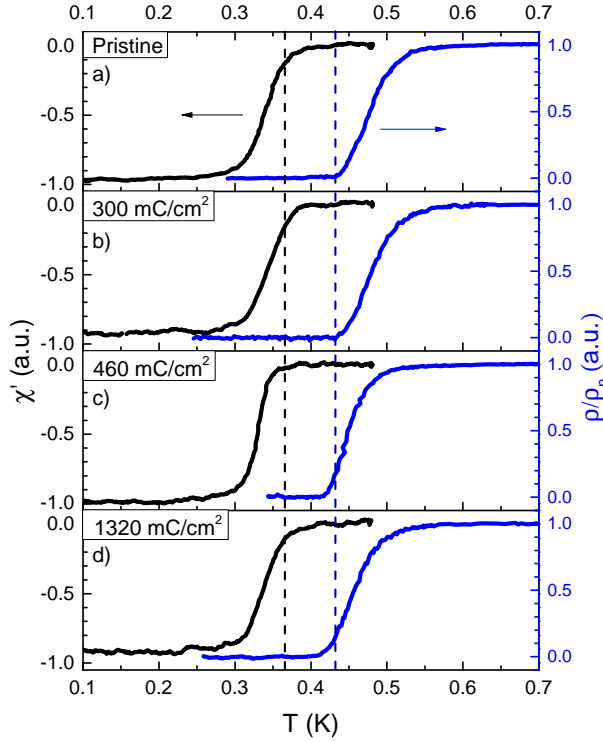


FIG. 2: The real part of ac susceptibility (χ') and normalized resistivity (ρ/ρ_n) as a function of temperature around T_c in absence of magnetic field for pristine and electron irradiated $\text{SrTi}_{0.987}\text{Nb}_{0.013}\text{O}_3$. Two vertical lines mark the transition temperatures in χ' and ρ/ρ_n . The superconducting transition barely shifts.

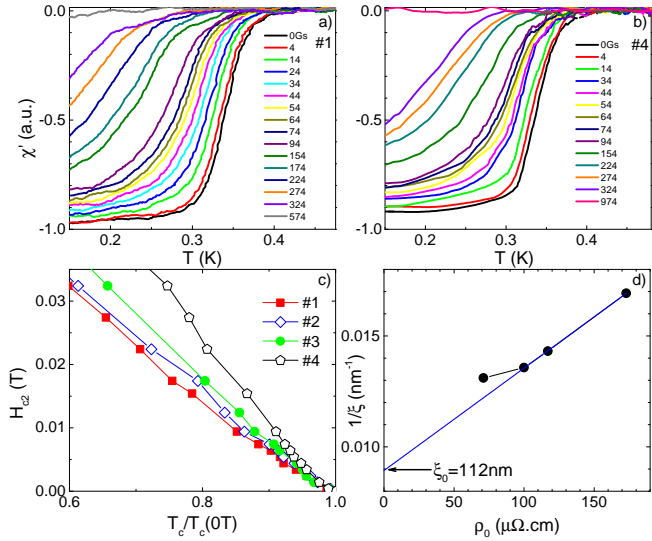


FIG. 3: The evolution of the upper critical field (H_{c2}) and the effective coherence length (ξ) with electron irradiation. a) and b) χ' as a function of temperature around the superconducting transition at different magnetic fields, for samples #1 and #4 respectively. c) The evolution of H_{c2} with $T_c/T_c(0T)$ from χ' . The slope of H_{c2} near T_c evolves with irradiation. d) $1/\xi$, as extracted from upper critical field, as a function of ρ_0 . The solid line is a linear fit.

tive coherence length (ξ) from this slope using the expression based on the Werthammer-Helfand-Hohenberg theory [37]:

$$1/\xi = \sqrt{\frac{2\pi\alpha}{\phi_0} T_c(0T) \frac{dH_{c2}}{dT} \Big|_{T=T_c(0T)}} \quad (1)$$

Here, ϕ_0 is the flux quanta and α is a dimensionless parameter ranging from 0.725 in the clean limit to 0.69 in the dirty limit. By assuming a dirty superconductor, the effective coherence length passes from 76 nm in the pristine sample #1 to 59 nm in the most irradiated sample #4 (see Table 1). Shortening the mean-free-path leads to a decreasing effective coherence length ξ . This is expected, since ξ can be expressed as:

$$1/\xi = 1/\xi_0 + 1/\beta \quad (2)$$

Here, ξ_0 is the intrinsic superconducting coherence length and β is the characteristic length of electrodynamic response of the normal state current. Pippard argued that the order of magnitude of β in a metal is the mean-free-path of electrons [38, 39]. Plotting $1/\xi$ as a function of ρ_0 in Fig. 3(d), one can extract an intercept, which yields $\xi_0 \sim 112$ nm. This is not far from the BCS coherence length (ξ_{BCS}), which can be estimated to be $\xi_{BCS} = \hbar v_F / \pi \Delta(0) \sim 140$ nm. The magnitude of the Fermi velocity, v_F is given by $\hbar k_F / m^*$ with $m^* = 4m_e$ [35], while the superconducting gap $\Delta(0K) \sim 80 \mu\text{eV}$ is inferred from early tunneling experiments [33]. We conclude that ξ_0 is larger than the mean-free-path in all samples, indicating that the single crystals in this study are dirty superconductors.

Interestingly, the magnitude of β derived using Eq. 2 is five to six times larger than the mean-free-path (see Table 1). This feature may be a peculiarity of this superconductor compared to those materials in which superconductivity emerges from a high carrier density metal. The huge electric permittivity in insulating SrTiO_3 leads to a long effective Bohr radius (a_B^*), as long as 700 nm [30], which is much larger than the mean-free-path. This may be the ultimate reason for a larger characteristic length for electrodynamic response in this low carrier density superconductor.

Let us compare our results with what has been reported in the case of other superconductors. Abrikosov and Gor'kov formulated a theory for the response of conventional superconductors to magnetic impurities [40]. According to this theory, T_c is suppressed, following:

$$-\ln\left(\frac{T_c}{T_{c0}}\right) = \psi\left(\frac{1}{2} + \frac{\alpha T_{c0}}{4\pi T_c}\right) - \psi\left(\frac{1}{2}\right) \quad (3)$$

Here, ψ is the digamma function, T_{c0} is the superconducting critical temperature in the clean limit, $\alpha = 2\hbar\tau_s/k_B T_{c0}$ is the dimensionless pair breaking parameter

TABLE 1: Irradiation dose (Q), superconducting critical temperature from ac susceptibility ($T_{c-\chi'}$) and resistivity ($T_{c-\rho}$) at zero field, residual resistivity at 2K (ρ_0), superconducting effective coherence length (ξ), mean-free-path (l), and the length scale (β) for pristine and electron-irradiated SrTi_{0.987}Nb_{0.013}O₃ single crystals.

| | #1 | #2 | #3 | #4 |
|------------------------|-------|-------|------|-------|
| $Q(mC/cm^2)$ | 0 | 300 | 460 | 1320 |
| $T_{c-sus}(K)$ | 0.37 | 0.372 | 0.35 | 0.368 |
| $T_{c-\rho}(K)$ | 0.435 | 0.435 | 0.42 | 0.419 |
| $\rho_0(\mu\Omega.cm)$ | 71 | 100 | 117 | 173 |
| $\xi(nm)$ | 76 | 74 | 70 | 59 |
| $l(nm)$ | 51 | 38 | 31 | 19 |
| $\beta(nm)$ | 240 | 215 | 186 | 125 |

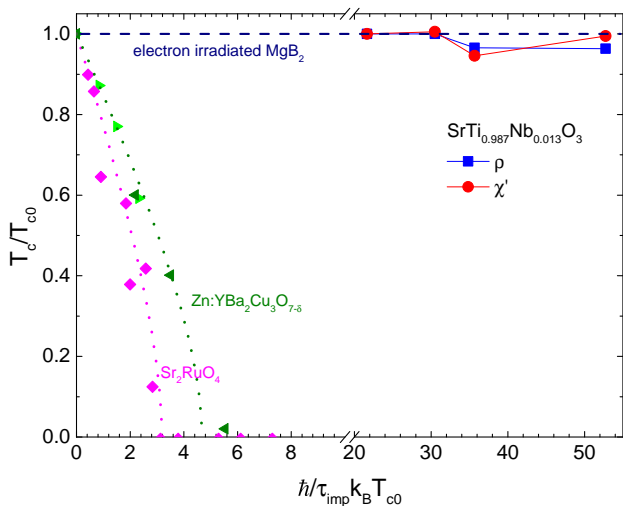


FIG. 4: T_c/T_{c0} as a function of the dimensionless pair-breaking rate $\alpha = \hbar\tau_{imp}/k_B T_{c0}$ in SrTi_{0.987}Nb_{0.013}O₃ determined from resistivity (■) and ac susceptibility (●). The data for MgB₂ under electron irradiation (the horizontal dashed line) is plotted for comparison, as well as those for two unconventional superconductors, Zn-doped cuprates (◀: YBa₂Cu₃O_{6.63}, ▶: YBa₂Cu₃O_{6.93}) and slightly disordered Sr₂RuO₄ (◆). The dotted lines are guides to the eyes. Superconductivity is robust against impurity scattering in SrTi_{0.987}Nb_{0.013}O₃ and in MgB₂, but is rapidly suppressed in the two unconventional superconductors.

and τ_s is the spin-flip scattering lifetime. Eq. 3 can be generalized to unconventional superconductors and their T_c evolution with non-magnetic potential scatter-

ing. This can be done by replacing α with $\hbar\tau_p/k_B T_{c0}$, in which τ_p is the potential scattering lifetime [3, 7, 8]. In order to make a simple comparison between experiment and theory, we take the residual resistivity as a measure of τ_p , taken to be equal to the transport life time τ_{imp} , expressed by $\tau_{imp} = \frac{m^*}{\rho n e^2}$.

Fig. 4 shows T_c/T_{c0} as a function of $\hbar\tau_{imp}/k_B T_{c0}$ (α) for SrTi_{0.987}Nb_{0.013}O₃, compared with three other superconductors. These are the conventional superconductor MgB₂ [16], as well as two unconventional superconductors YBa₂Cu₃O_{7- δ} (d-wave) [2] and Sr₂RuO₄ (p-wave) [5], which are both perovskites like the system under study. In both YBa₂Cu₃O_{7- δ} and Sr₂RuO₄, T_c is extremely sensitive to the introduction of disorder and superconductivity is completely destroyed when α exceeds a number of the order of unity. In contrast, superconductivity in SrTi_{0.987}Nb_{0.013}O₃ is robust and T_c shows a negligible variation even when α becomes very large. A similar behavior was observed in MgB₂. This is strong evidence for s-wave superconductivity in SrTi_{0.987}Nb_{0.013}O₃ and the main conclusion of this study.

In summary, performing resistivity and ac susceptibility measurements on electron irradiated optimally doped SrTi_{0.987}Nb_{0.013}O₃, we have found that superconductivity is robust against impurity potential scattering deep into the dirty limit ($\xi_0/l \sim 5.9$). In addition, we have quantified the intrinsic clean coherence length (ξ_0) and found that it is comparable to the BCS coherence length (ξ_{BCS}). Combined with the thermal conductivity data, which pointed to the absence of nodal quasi-particles [35], this result identifies SrTi_{1-x}Nb_xO₃ as a multi-gap s-wave superconductor. The negligible suppression of T_c also indicates that the relative weight of inter-band and intra-band scattering is not altered by electron irradiation. In oxygen deficient SrTiO₃ with a carrier concentration 400 times lower than the samples studied here, the Fermi energy becomes one order of magnitude lower than the Debye temperature, a serious challenge for a phonon-mediated pairing mechanism [30]. Further experiments are required to probe the evolution of the gap symmetry and the pairing mechanism in a system whose superconductivity survives over three-orders-of-magnitude of carrier concentration.

We thank the staff of the SIRIUS accelerator for technical support. This work is supported by Agence Nationale de la Recherche as part of SUPERFIELD project.

[1] P. W. Anderson, J. Phys. Chm. Solids **11**, 26 (1959).
[2] Y. Fukuzumi, K. Mizuhashi, K. Takenaka, and S. Uchida, Phys. Rev. Lett. **76**, 648 (1996).
[3] Sergey K. Tolpygo, J.-Y. Lin, and Michael Gurvitch, S. Y. Hou, and Julia M. Phillips, Phys. Rev. B **53**, 12454 (1996).
[4] F. Rullier-Albenque, P. A. Vieillefond, H. Alloul, A. W.

Tyler, P. Lejay, and J. F. Marucco, Europhys. Lett. **50**, 81 (2000).
[5] A. P. Mackenzie, and Y. Maeno, Rev. Mod. Phys. **75**, 657 (2003).
[6] J. S. Kim, D. Bedorf, and G. R. Stewart, J. Low Temp. Phys. **157**, 29 (2009).
[7] R. J. Radtke, K. Levin, H. B. Schüttler, and M. R. Nor-

- man, Phys. Rev. B **48**, 653 (1993).
- [8] Abrikosov, Physica C **214**, 107 (1993).
- [9] A. J. Millis, S. Sachdev, and C. M. Varma, Phys. Rev. B **37**, 4975 (1988).
- [10] L. S. Borkowski, and P. J. Hirschfeld, Phys. Rev. B **49**, 15 404 (1994).
- [11] R. Prozorov, M. Kończykowski, M. A. Tanatar, A. Thaler, S. L. Budko, P. C. Canfield, V. Mishra, and P. J. Hirschfeld, Phys. Rev. X **4**, 041032 (2014).
- [12] A. A. Golubov, and I. I. Mazin, Phys. Rev. B **55**, 15146 (1997).
- [13] Y. Wang, A. Kreisel, P. J. Hirschfeld, and V. Mishra, Phys. Rev. B **87**, 094504 (2013).
- [14] F. Rullier-Albenque, H. Alloul, and R. Tourbot, Phys. Rev. Lett. **87**, 157001 (2001).
- [15] A. Legris, F. Rullier-Albenque, E. Radeva, and P. Lejay, J. Phys. I (France) **3**, 1605 (1993).
- [16] A. A. Blinkin, V. V. Derevyanko, A. N. Dovbnya, T. V. Sukhareva, V. A. Finkel, and I. N. Shlyakhov, Phys. Solid State **48**, 2037 (2006).
- [17] T. Klein, R. Marlaud, C. Marcenat, H. Cercellier, M. Konczykowski, C. J. van der Beek, V. Mosser, H. S. Lee, and S. I. Lee, Phys. Rev. Lett. **105**, 047001 (2010).
- [18] A. A. Blinkin, V. V. Derevyanko, T. V. Sukhareva, V. L. Uvarov, V. A. Finkel, Yu. N. Shakhov, and I. N. Shlyakhov, Phys. Solid State **53**, 245 (2011).
- [19] R. H. T. Wilke, S. L. Budko, P. C. Canfield, J. Farmer, and S. T. Hannahs, Phys. Rev. B **73**, 134512 (2006).
- [20] R. Gandikota, R. K. Singh, J. Kim, B. Wilkens, N. Newman, J. M. Rowell, A. V. Pogrebnikov, X. X. Xi, J. M. Redwing, S. Y. Xu, and Q. Li, Appl. Phys. Lett. **86**, 012508 (2005).
- [21] M. Putti, R. Vaglio, and J. M. Rowell, Supercond. Sci. Technol. **21**, 043001 (2008).
- [22] L. Civale, A. D. Marwick, T. K. Worthington, M. A. Kirk, J. R. Thompson, L. Krusin-Elbaum, Y. Sun, J. R. Clem, and F. Holtzberg, Phys. Rev. Lett. **67**, 648 (1991).
- [23] W. Gerhäuser, G. Ries, H. W. Neumüller, W. Schmidt, O. Eibl, G. Saemann-Fschenko, and S. Klaumünzer, Phys. Rev. Lett. **68**, 879 (1992).
- [24] Y. Nakajima, Y. Tsuchiya, T. Taen, T. Tamegai, S. Okayasu, and M. Sasase, Phys. Rev. Lett. **80**, 012510 (2009).
- [25] A. C. Damask and G. J. Dienes, Point Defects in Metals (Gordon & Breach Science Publishers Ltd, London, 1963).
- [26] K. A. Müller, and H. Burkard, Phys. Rev. B **19**, 3593 (1979).
- [27] D. van der Marel, J. L. M. van Mechelen, and I. I. Mazin, Phys. Rev. B **84**, 205111 (2011).
- [28] J. F. Schooley, W. R. Hosler, E. Ambler, J. H. Becker, Marvin L. Cohen, and C. S. Koonce, Phys. Rev. Lett. **14**, 305 (1965).
- [29] C. S. Koonce, Marvin L. Cohen, J. F. Schooley, W. R. Hosler, and E. R. Pfeiffer, Phys. Rev. **163**, 380 (1967).
- [30] X. Lin, Z. W. Zhu, B. Fauqué, and K. Behnia, Phys. Rev. X **3**, 021002 (2013).
- [31] J. F. Schooley, W. R. Hosler, and Marvin L. Cohen, Phys. Rev. Lett. **12**, 474 (1964).
- [32] X. Lin, G. Bridoux, A. Gourgout, G. Seyfarth, S. Krämer, M. Nardone, B. Fauqué, and Kamran Behnia, Phys. Rev. Lett. **112**, 207002 (2014).
- [33] G. Binnig, A. Baratoff, H. E. Hoening, and J. G. Bednorz, Phys. Rev. Lett. **45**, 1352 (1980).
- [34] C. Richter, H. Boschker, W. Dietsche, E. Fillis-Tsirakis, R. Jany, F. Loder, L. F. Kourkoutis, D. A. Muller, J. R. Kirtley, C. W. Schneider, and J. Mannhart, Nature **502**, 528 (2013).
- [35] X. Lin, A. Gourgout, G. Bridoux, F. Jomard, A. Pourret, B. Fauqué, D. Aoki, and K. Behnia, Phys. Rev. B **90**, 140508(R) (2014).
- [36] G. L. Cheng, M. Tomczyk, S. C. Lu, J. P. Veazey, M. C. Huang, P. Irvin, S. Ryu, H. Lee, C. B. Eom, C. S. Hellberg, and J. Levy, Nature **521**, 196 (2015).
- [37] E. Helfand, and N. R. Werthamer, Phys. Rev. **147**, 288 (1966); N. R. Werthamer, E. Helfand, and P. C. Hohenberg, Phys. Rev. **147**, 295 (1966).
- [38] A. B. Pippard, Proc. Roy. Soc. (London) **A216**, 547 (1953).
- [39] M. Tinkham, Introduction to Superconductivity (McGraw-Hill, New York, 1975).
- [40] A. A. Abrikosov, and L. P. Gorkov, Sov. Phys. JETP **12**, 1243 (1961).